Results in Engineering 16 (2022) 100654

Contents lists available at ScienceDirect

Results in Engineering

journal homepage: www.sciencedirect.com/journal/results-in-engineering

Application of the arithmetic optimization algorithm to solve the optimal power flow problem in direct current networks

Jhon Montano [a,*], Oscar Daniel Garzón [b], Andrés Alfonso Rosales Muñoz [c], L.F. Grisales-Noreña [c], Oscar Danilo Montoya [d,e]

[a] Department of Electronics and Telecommunications, Instituto Tecnológico Metropolitano, Medellín 050028, Colombia
[b] Electrical and Computer Engineering Department, University of Puerto Rico at Mayaguez, Mayaguez, PR 00680, USA
[c] Grupo MATyER, Facultad de Ingeniería, Instituto Tecnológico Metropolitano, Campus Robledo, Medellín 050036, Colombia
[d] Facultad de Ingeniería, Universidad Distrital Francisco José de Caldas, Carrera 7 No. 40B - 53, Bogotá D.C 11021, Colombia
[e] Laboratorio Inteligente de Energía, Universidad Tecnológica de Bolívar, km 1 via Turbaco, Cartagena, 131001, Colombia

ARTICLE INFO

Keywords:
Optimal power flow
Power flow
Optimization algorithms
DC networks
Electric power
Optimization

ABSTRACT

This article presents a methodology to solve to the Optimal Power Flow (OPF) problem in Direct Current (DC) networks using the Arithmetic Optimization Algorithm (AOA) and Successive Approximation (SA). This master-slave methodology solves the OPF problem in two stages: the master stage estimates the solution to the OPF problem considering its constraints and variables, and the slave stage assesses the fitness of the solution proposed by the master stage. To validate the methodology suggested in this article, three test systems cited multiple times in the literature were used: the 10, 21 and the 69 nodes test systems. In addition, three scenarios varying the allowable power limits for the Distributed Generators (DGs) are presented; thus, the methodology explores solutions under different conditions. To prove its efficiency and robustness, the solution was compared with four other methods reported in the literature: Ant Lion Optimization (ALO), Black Hole Optimization (BHO), the Continuous Genetic Algorithm (CGA), and Particle Swarm Optimization (PSO). The results show that the methodology proposed here to reduce power losses presents the best solution in terms of standard deviation.

1. Introduction

Microgrids are defined as micro- and macro-scale systems that can operate with both Alternating Current (AC) and Direct current (DC) in isolated systems or connected to a power grid. Their implementation in DC networks is well-known because they can be used to integrate distributed energy resources [1]. Non-conventional energy sources are one of the most important resources nowadays because they reduce CO_2 emissions significantly by decreasing the production of electric power from fossil fuels. Due to the relevance of DC networks today, the scientific community has identified the need to study ways to improve their technical-economical aspects and increase their efficiency [2,3]. As a result, it has been found that integrating Distributed Generators (DGs) into DC networks can improve their behavior and performance considerably—which is known as Optimal Power Flow (OPF) and can be used to study and optimize several network-related problems. However, some of their most frequent technical operating difficulties are electric power losses, CO_2 emissions, network operating costs, and out-of-limit voltage profiles and current [4–6]. An overview of DC networks and the OPF is presented below.

1.1. DC networks and the power flow problem

Due to the progress made and the results obtained in power electronics, it is possible to transmit and distribute energy as direct current [7]. DC networks have advantages over their alternating current counterparts, e.g., phasors and reactive components; hence, they make it easy to calculate their characteristic power variables. They also eliminate the use of AC/DC converters, thus reducing power losses by conversion [8–10].

DC networks are usually composed of one slack generator (sometimes two), distribution lines, constant power loads, distributed generators, and power storage devices [11,12]. To design them, after the DC network and its components have been determined, it is necessary to

* Corresponding author.
E-mail addresses: jhonrojas@itm.edu.co (J. Montano), oscar.garzon@upr.edu (O.D. Garzón), andresrosales224822@correo.itm.edu.co (A.A. Rosales Muñoz), luisgrisales@itm.edu.co (L.F. Grisales-Noreña), odmontoyag@udistrital.edu.co, omontoya@utb.edu.co (O.D. Montoya).

https://doi.org/10.1016/j.rineng.2022.100654
Received 3 June 2022; Received in revised form 2 September 2022; Accepted 19 September 2022
Available online 24 September 2022

establish the amount of power that DGs should inject into the grid to improve network operation and thus obtain economic, operating, technical, and environmental benefits [7]. The objective of OPF is to improve the objective function set by the network operator. Here, the objective function is the reduction of power losses (*Ploss*) associated with power distribution considering that it has been widely used in the specialized literature, according to a state-of-the-art review [13].

1.2. The OPF problem in DC networks: state of the art

Multiple investigations have focused on the OPF problem in DC networks in recent years. They have proposed solutions such as the implementation of algorithms based on commercial software and sequential programming models using optimization techniques and numerical methods. The optimal power value that DGs in a network should inject to comply with regulations and to minimize power losses can be determined employing these solutions [14].

Regarding the OPF solution methodology using commercial software, in Refs. [15–17], the objective function is to minimize power losses associated with power distribution. Due to the solution methodology used in this paper, it is not possible to replicate the ones proposed by those authors because they used commercial software. In Ref. [15], the convex relaxation method based on second-order conic programming is used by means of *MOSEK*, which is commercial software. In that paper, the OPF problem is solved for a 16-bus DC network considering processing times and standard deviation. In Ref. [16], sequential convex programming is used to solve the OPF problem for 10- and 21-bus test systems considering processing times but not standard deviation. In Ref. [17], *GAMS/CONOPT* and the continuous genetic algorithm are used to assess the OPF problem for a 10-bus test system, comparing the solution obtained by the proposed methodology and the one obtained by *GAMS*; however, the processing times and the standard deviation are not considered. The cited studies used commercial software and small DC networks (10, 16, and 21 buses); thus, it is not possible to establish the robustness of those methodologies. Besides, they did not consider the currents flowing through the power lines, the worst voltage in the system, and other parameters necessary to establish network performance.

Aiming to promote the use of open source software and eliminate the use of its commercial counterpart, new sequential programming methods based on optimization algorithms and numerical methods have been suggested to solve the OPF problem; for instance, in Refs. [18–20]. These techniques implement a master-slave solution methodology, where the optimization algorithm is the master stage, and a numerical method selected to solve the power flow problem is the slave stage. In Ref. [18], the multiverse optimization algorithm is used as the master stage, and Successive Approximation (SA) as the slave stage. That paper proposes a solution to the OPF problem for the 21- and 69-bus test systems, considering the currents flowing through the lines but disregarding processing times. In Ref. [19], the sine cosine algorithm is proposed as the master stage; and SA, as the slave stage. In that article, the solution to the OPF problem is proposed only for the 21-bus system, the currents flowing through the lines are not considered, and the processing times and standard deviation obtained by the optimization algorithms are disregarded. In Ref. [1], the authors propose a master-slave methodology combining the Ant Lion Optimization (ALO) algorithm and SA to solve the OPF problem in 21- and 69-bus systems, considering processing times but disregarding the standard deviation. Some of the articles that suggest the use of open source software do not analyze the computation time required by the methodologies; then, it is not possible to determine the methodology's performance. Also, among the cited papers, tuning is performed in only one, i.e., [18]; therefore, the techniques are not implemented under the same operating conditions.

After the state-of-the-art review above, we conclude that new techniques should apply sequential programming and encourage the use of open source software to solve the OPF problem. Additionally, new studies should detail the tuning of the techniques that produce high quality solutions and low processing times, as well as the standard deviation of the optimization algorithms and the currents flowing through the lines, which were not considered in some studies.

Hence, this paper proposes a new optimization technique based on a master-slave methodology where the master stage uses the AOA and the slave stage is performed by the SA. This methodology proposes a solution for the 21- and 69-bus test systems with distributed generation of 20%, 40%, and 60% of the power provided by the slack generator. The solution quality, processing time, and robustness of the solution methodology are thoroughly analyzed.

1.3. Scope and contributions

This document addresses the OPF problem from the viewpoint of sequential programming methodologies, thus avoiding the use of commercial software, and proposes the application of the AOA combined with SA. The purpose is to generate a highly effective hybrid methodology in terms of quality and time. The following are the main contributions of this paper to the state of the art:

- A new application for the arithmetic optimization algorithm.
- A new master-slave methodology that solves the OPF problem in DC networks.
- Better results (in terms of quality, repeatability, and computation times) than those of other methodologies that have been implemented to solve the OPF problem in DC networks.

1.4. Structure of the article

This paper is organized as follows. Section 2 presents the mathematical formulation of the OPF problem in DC networks, where the objective function is the reduction of power losses associated with power distribution considering all the constraints of DC networks in a distributed generation environment. Section 3 introduces the proposed optimization technique to solve the OPF problem applying a master-slave methodology that combines the AOA and SA. Section 4 details the optimization algorithms that are compared with the proposed solution methodology, as well as the test systems used to perform the simulations. Section 5 reports the results obtained by the optimization algorithms for the 10, 21 and 69 nodes test systems at different percentages of distributed power penetration. Finally, Section 6 draws the conclusions and suggests future research.

2. Mathematical formulation

The state-of-the-art review above shows that the solution to the OPF problem is related to the power flow and the constraints set by the network operator [21]. Once they are established, it is possible to determine the stability of the system, the current congestion in the lines, and the power losses, among others. Thus, in this case study, the power losses are the variable of interest, and the objective function is to minimize them. The equations that compose the objective function and the OPF constraints are presented below.

2.1. Objective function

The objective function is defined as a specific problem to be solved or minimized by applying an optimal flow. This paper addresses the reduction of power losses in a DC network.

$$minP_{loss} = v^T G_L v \tag{1}$$

In Equation (1), P_{loss} represents the function to be reduced, that is, the power losses in the system as a function of v, which is a vector containing all the voltage profiles calculated using the load flow; and G_L is the matrix that represents the conductivity effects of each line.

2.2. Constraints

This subsection details the set of equations that represent the constraints of the OPF problem. They refer to the technical and operational issues that should be considered to obtain an optimal and viable solution to the OPF problem. These equations and their details are presented below:

$$P_g + P_{DG} - P_d = D(v)[G_L + G_N]v, \tag{2}$$

$$P_g^{min} \leq P_g \leq P_g^{max}, \tag{3}$$

$$P_{DG}^{min} \leq P_{DG} \leq P_{DG}^{max}, \tag{4}$$

$$v^{min} \leq v \leq v^{max}, \tag{5}$$

$$I_{ij} \leq I_{ij}^{max}, \tag{6}$$

$$1^T(P_{DG} - \alpha P_g) \leq 0, \tag{7}$$

The mathematical interpretation of Equations (2)–(7) is the following. In Equation (2), the main factors, P_g, P_{DG}, and P_d, are the power generated by the slack node, the power supplied by the DGs, and the power demanded by the network nodes, respectively. This equation expresses the power balance of the network. In Equation (2), $D(v)$ is a positive symmetric matrix whose diagonal contains the nodal voltages of the system, while G_L and G_N represent the inductive and resistive components of the microgrid lines, respectively. Equations (3) and (4) contain P_g^{min} and P_g^{max}, which denote the minimum and maximum power that the slack node can supply to the network. Likewise, P_{DG}^{min} and P_{DG}^{max} define the minimum and maximum power that the DGs can supply. Equations (3) and (4) determine and limit the power to be injected into the microgrid, both the power coming from the main generator located in the slack node and that supplied by the DGs, in such a way that there are no power losses due to over injection. Equation (5) includes $v^{\min}$ and $v^{\max}$, which define the maximum and minimum allowable voltage. This constraint ensures that the voltages resulting after power injection comply with voltage regulations, avoiding sags and swells that destabilize the system. One of the limits that facilitate a stable system is Equation (6) because it contains the current flowing through the lines, I_{ij}, which must be lower than I_{ij}^{max}. Finally, Equation (7) defines the maximum penetration of DG, where α represents the allowable percentage of penetration with respect to the power generated by the slack node.

3. Proposed methodology

The equations introduced in Section 2 represent the objective function and the constraints of the OPF problem. From the state of the art in Subsection 1.2, we conclude that, to address this problem, it is necessary to analyze the behavior of OPF methods. Therefore, since it involves power flows, the OPF problem is non-linear-non-convex, and it is necessary to use numerical methods and metaheuristic techniques to solve it. This article presents an optimization algorithm that solves the OPF problem in two stages. First, the master stage is carried out using the AOA proposed in Ref. [22]. Second, in the slave stage, SA is used to solve the power flow [23], and the proposed objective function is evaluated. In this master-slave methodology, the problem is solved in two stages that operate together. The two methods, the AOA and SA, were selected for this study based on the excellent results of each method independently, according to the literature reviewed above.

3.1. Master stage: arithmetic optimization algorithm

The AOA is a technique inspired by the distribution behavior of the main arithmetic operators in mathematics, which is based on the principles of modern mathematics, geometry, and algebra. Arithmetic uses the four basic mathematical operations (i.e., addition, subtraction, multiplication, and division) to study numerical methods employed to solve any problem using mathematical optimization. In other words, the AOA is useful to establish the best solution to an optimization problem by generating a population and using arithmetic operators hierarchically according to the domain of the optimization algorithms. This gives the AOA the possibility of creating a population (with a search space) that applies two fundamental strategies: exploration and exploitation. In the former, search agents expand the search space to solve a specific problem while avoiding local solutions. In the latter, they improve the accuracy of the solutions obtained in the previous phase. Therefore, these two search mechanisms (Fig. 1) use the arithmetic operators hierarchically as follows: Division (D "÷"), Multiplication (M "*"), Subtraction (S" − "), and Addition (A" + "). The next subsection presents the phases of computational development and those used here to solve the OPF problem implementing the AOA.

3.1.1. Generation of the initial population

Equation (8) is used to create the initial population ($Xi(i,j)$), where each Xi in the population represents a possible solution to the problem. Subscript i in the initial population denotes the i-th individual, and subscript j is the j-th dimension of the problem that denotes each i element. In the OPF problem, each individual generated in the different dimensions represents an amount of power to be injected by the DGs into the DC network. Each individual has a value given within the solution space and limited by the technical constraints of the problem. The value is a result of implementing upper (ub) and lower (lb) bounds assigned to the dimensions of the problem, which correspond to the maximum and minimum power level assigned to each generator in the OPF problem. The first population is generated from random values ($rand$) in the [0 − 1] range to explore larger regions in the search space. They are multiplied by the difference between the limits, thus allowing a greater distribution of individuals within the search space.

$$Xi_{(i,j)} = ((ub - lb) * rand) + lb \tag{8}$$

The previous equation determines the values of individuals i in dimension j. To create the entire population of individuals Xi, we propose a size nxd matrix, where n represents the number of individuals as viable solutions to the problem, and d represents the number of variables. In Equation (9), X_n is the n-th individual in matrix M_{Xi}. In the OPF problem, the total number of columns d is the number of DGs in the DC network (other than the slack node), and the value in each column is the power they inject into the network.

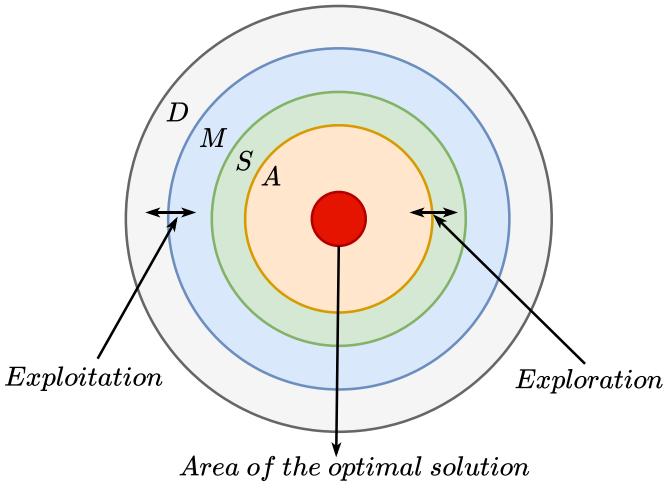

Fig. 1. Hierarchical order of arithmetic operators.

$$M_{Xi} = \begin{bmatrix} Xi_{1,1} & Xi_{1,2} & \cdots & \cdots & Xi_{1,d} \\ Xi_{2,1} & Xi_{2,2} & \cdots & \cdots & Xi_{2,d} \\ \vdots & \vdots & \vdots & \vdots & \vdots \\ \vdots & \vdots & \vdots & \vdots & \vdots \\ Xi_{n,1} & Xi_{n,2} & \cdots & \cdots & Xi_{n,d} \end{bmatrix} = \begin{bmatrix} Xi_1 \\ Xi_2 \\ \vdots \\ \vdots \\ Xi_n \end{bmatrix} \quad (9)$$

3.1.2. Calculation of the objective function

The slave stage evaluates the objective function of each individual (fitness function) and then assesses the impact of the viable solutions contained in M_{Xi}. Each value is stored in a $nx1$ matrix called MO_{Xi}, and the losses in the power injected by each DG are calculated (see Equation (10)). In the OPF problem, each individual generated in the search space and assigned to each Xi is evaluated and the values of the variables for each possible solution are obtained.

$$MO_{Xi} = \begin{bmatrix} f\left(\left[X_{1,1}, X_{1,2}, \ldots, X_{1,d}\right]\right) \\ f\left(\left[X_{2,1}, X_{2,2}, \ldots, X_{2,d}\right]\right) \\ \vdots \\ f\left(\left[X_{n,1}, X_{n,2}, \ldots, X_{n,d}\right]\right) \end{bmatrix} \quad (10)$$

The individuals with the best solution in the MO_{Xi} matrix (i.e., lowest power losses) are selected as the incumbent solution. Then, the objective function is stored in Equation (9), and the configuration of its variables during the iterative cycle are stored in Equation (10). To establish the best solution at the current iteration, this study proposes comparing the solutions stored in the solutions vector given by the objective function. If a better solution than the incumbent is obtained at a certain iteration, the *Best_Fob* and *Best_Xi* values are updated. In Equation (12), *Best_Xi* is a vector of $1xd$, and a denotes the individuals that represent the best objective function at each iteration.

$$Best\_Fob = \left[f\left(Xi_{1,d}\right)\right] \quad (11)$$

$$Best\_Xi = [X_a] \quad (12)$$

3.1.3. Exploration and exploitation phases

The AOA applies an iterative process using arithmetic operators according to the phase: exploration and exploitation (i.e., the movement method of the optimization technique). The exploration phase uses the Division (D) and Multiplication (M) operators, which obtain decision values under a high dispersion rate and compromise the exploitation phase. Note that operators D and M cannot easily approach a feasible solution due to their high dispersion, unlike Addition (A) and Subtraction (S), which are used in the exploitation phase and can easily approach a feasible solution. A and S can be used to start each search phase, which depends on a starting point obtained by calculating Equation (13), also known as the Math Optimizer Accelerated (MOA). In other words, exploration and exploitation are used to generate all the new individuals in the iterative process in each particle and dimension of the problem.

$$MOA = Min + Cont \times \left(\frac{Max - Min}{Maxiter}\right) \quad (13)$$

This equation determines which phase will be executed in the iterative process in the AOA (i.e., exploration or exploitation). Here, *Cont* denotes the current iteration, ranging from an initial value of 1 to the maximum number of iterations, i.e., *Maxiter*. The value defined as the minimum of the accelerated function ($Min = 0.2$) and the maximum value ($Max = 1$) enable the MOA to determine a value to compare it with a random value, i.e., $r1$. The process advances as follows: if ($r1 < MOA$), the exploration phase is used; otherwise, the exploitation phase is employed. The two phases are described below:

- **Exploration phase:** It uses D and M to conduct a stochastic search. These two operators, which are its main search strategies, are modeled in Equation (14).

$$Xi_{(i,j)} = \begin{cases} Best\_Xi \times MOP \times \left(\left(ub_{(1,j)} - lb_{(1,j)}\right) \times \mu + lb_{(1,j)}\right) & r2 < 0.5 \\ \dfrac{Best\_Xi}{(MOP + \varepsilon)} \times \left(\left(ub_{(1,j)} - lb_{(1,j)}\right) \times \mu + lb_{(1,j)}\right) & r2 > 0.5 \end{cases} \quad (14)$$

This equation depends on a random value, $r2$, in the $[0 - 1]$ range. This value allows determining the phase to be used, that is, if ($r2 < 0.5$), the M operator is used. Therefore, the exploration phase is based on Equation (14), using the individuals (*Best_Xi*) who provided the best solution so far employing the Math Optimizer Probability (*MOP*), the upper bounds (*ub*), lower bounds (*lb*), and a fixed value ($\mu = 0.5$), which is a parameter to control the search fitness. If the opposite occurs (i.e., $r2 > 0.5$), the D operator will be implemented using the best individuals, the upper and lower bounds, the MOP, and a parameter $\epsilon = 2.2204e^{-16}$.

$$MOP = 1 - \frac{cont^{1/\alpha}}{Maxiter^{1/\alpha}} \quad (15)$$

In Equation (15), MOP is a coefficient expressed as the value of the function at the present iteration, the maximum number of iterations, and a parameter $\alpha = 5$ that determines the accuracy of the exploration phase throughout the iterative process [22].

- **Exploitation phase:** This search phase uses Addition (A) and Subtraction (S) to take advantage of the search space because these operators make it easy to approach a solution due to the low dispersion of their search mechanism. Thus, the aim of the exploitation phase is to determine the most optimal solution (among the given solutions) at each iteration using Equation (16).

$$Xi_{(i,j)} = \begin{cases} Best\_Xi \times MOP + \left(\left(ub_{(1,j)} - lb_{(1,j)}\right) \times \mu + lb_{(1,j)}\right) & r3 < 0.5 \\ Best\_Xi \times MOP - \left(\left(ub_{(1,j)} - lb_{(1,j)}\right) \times \mu + lb_{(1,j)}\right) & r3 > 0.5 \end{cases} \quad (16)$$

This equation, like the exploration phase, depends on a random value, $r3$, in the $[0 - 1]$ range. If ($r3 < 0.5$), S is used to perform the exploitation based on Equation (16). The latter uses the individuals who provided the best solution obtained so far (*Best_Xi*) employing the *MOP*, the addition of upper bounds (*ub*), lower bounds (*lb*), and parameter μ. If ($r3 > 0.5$), R is used following the same process, but doing a subtraction.

Once the phase to be used is determined and it is applied to the current iteration, the position of each individual in the iterations is updated, making sure they respect the constraints of the problem; in this case, not exceeding the power values set for the DGs. Subsequently, MO_{Xi} is updated by assessing the new individuals according to the objective function and updating the incumbent problem at each iteration. This process is repeated until the stopping criteria established for this problem are met.

3.1.4. Stopping criteria

The two stopping criteria used in the master stage are described below:

- The master stage will end after n consecutive iterations if the incumbent of the problem is not updated. That is, the iterative process ends when the objective function reaches a considerable number of iterations (a non-improvement counter) without finding a better solution to the problem.
- The computation ends when the optimization algorithm reaches the maximum allowable number of iterations, which is controlled by a counter in the algorithm.

The iterative process in Algorithm 1 is presented below to help readers understand the proposed AOA-SA solution methodology.

Algorithm 1
Hybrid AOA-SA optimization algorithm

1:Load system data
2:Initialize the parameters of the algorithms
3:Generate initial population of individuals (M_{Xi})
4:Calculate adaptation function employing slave stage (MO_{Xi})
5:Select the incumbent solution (*Best_Fob*)
6:Select the best individuals (*Best_Xi*)
7:Initialize *P*, *Max*, and *Min* parameters
8:**while** $Cont \leq Maxiter$ **do**
9: Initialize *MOP* view (15)
10: Initialize *MOA* view (13)
11: **for** $(i = 1 : Size(Xi))$ **do**
12: **for** $(j = 1 : Dim)$ for dimension of the problem **do**
13: $r1 = rand\ [0 - 1]$
14: **if** $r1 < MOA$ **then**
15: $r2 = rand\ [0 - 1]$
16: **if** $r2 < MOA$ **then**
17: $Xi_{(i,j)} = Best\_Xi \times MOP \times \left(\left(ub_{(1,j)} - lb_{(1,j)}\right) \times \mu + lb_{(1,j)}\right)$
18: **else**
19: $Xi_{(i,j)} = \frac{Best\_Xi}{(MOP + \varepsilon)} \times \left(\left(ub_{(1,j)} - lb_{(1,j)}\right) \times \mu + lb_{(1,j)}\right)$
20: **end if**
21: **else**
22: $r3 = rand\ [0 - 1]$
23: **if** $r3 < 0.5$ **then**
24: $Xi_{(i,j)} = Best\_Xi \times MOP + \left(\left(ub_{(1,j)} - lb_{(1,j)}\right) \times \mu + lb_{(1,j)}\right)$
25: **else**
26: $Xi_{(i,j)} = Best\_Xi \times MOP - \left(\left(ub_{(1,j)} - lb_{(1,j)}\right) \times \mu + lb_{(1,j)}\right)$
27: **end if**
28: **end if**
29: **end for**
30: **end for**
31: Calculate adaptation function by means of *SA*
32: Update incumbent solution
33: $Cont = Cont + 1$;
34:**end while**

3.2. Slave stage

The slave stage assesses the fitness of the solution suggested by the master stage and solves the power flows to determine if the suggested power injections for the DGs are adequate. The slave stage—in which the objective function is evaluated—should be fast, accurate, and effective because optimization algorithms should be efficient.

This paper suggests solving the OPF problem using an iterative method based on SA [23], which was selected due to the convergence of its solution and its short processing time. This method is based on the following equation:

$$G_{dd} \cdot v_d = -D_d^{-1}(v_d) P_d - G_{dg} \cdot v_g \tag{17}$$

where G_{dd} is a positive symmetric matrix containing all the conductivity effects of the distribution lines; v_g, the voltage profile of the slack node; and v_d, the voltage at demand nodes. Through a mathematical development applied to Equation (17), it is possible to get a new equation and establish the nodal voltages at demand nodes.

$$v_d = -G_{dd}^{-1}[D_d^{-1}(v_d) P_d + G_{dg} \cdot v_g] \tag{18}$$

To find these values in the v_d system, an iterative process should be implemented to find the nodal voltages with an almost null convergence error. Thus, a t counter should be implemented in Equation (18). The following is the equation to find the voltage profiles:

$$v_d^{t+1} = -G_{dd}^{-1} D_d^{-1}(v_d^t) P_d + G_{dg} \cdot v_g \tag{19}$$

To explain the master-slave methodology in detail, which aims to reduce the power losses in DC networks, in Fig. 2 is presented the flowchart of the methodology describe in this research document. The flowchart presents all step necessaries to execute the optimization algorithm and obtain the solution to OPF problem. The steps presented in the flowchart are described below:

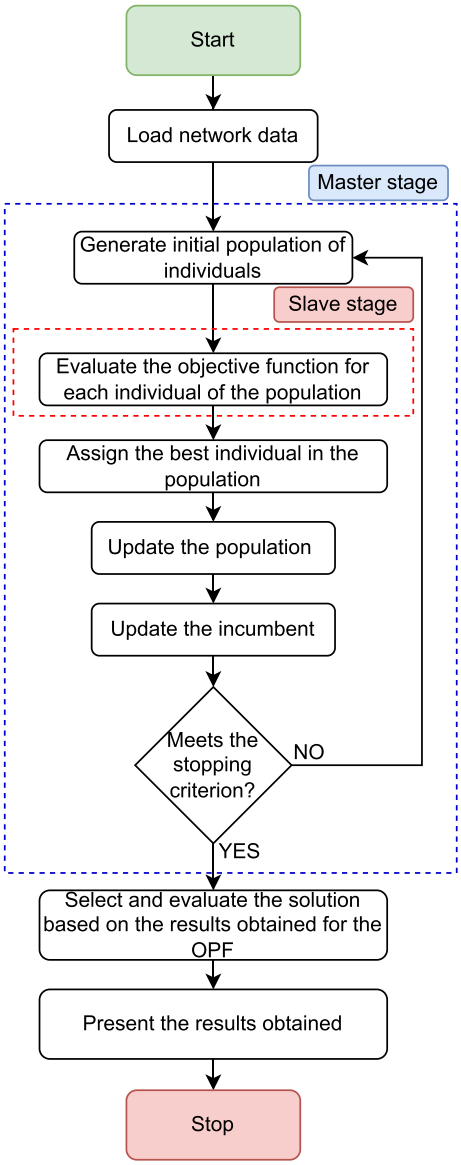

Fig. 2. Hybrid AOA-SA optimization algorithm diagram.

The proposed methodology required that, first: the data of the electrical system must be load and the initial condition that represent the OPF problem in DC networks, must be load too. The data correspond to electrical parameters, nodes connections, resistive in the branch, percentage of power penetration (α), optimization algorithm parameters, among others. Second: the master stage (AOA) begins, in this stage is generate the initial popualtion, next the stage slave evaluate the objetive funcion for each particle in the initial population and the best incumbent is assigned for the firts population. Third: Based on the incumbent and the initial parameters, the population is updated. Fourth: checks if any of the stop criteria are met. Fifth: once a stop criterion is met, the optimization algorithm stops and the results obtained are presented. It should be noted that these iterative processes are run over and over again until the stop criteria are met in their entirety and when this occurs the best result obtained for the OPF is selected and these results are presented.

4. Test scenarios and considerations

In this study, three test systems were used to validate the proposed

methodology. The systems were adapted from previous versions in AC and based on the state of the art.

To adapt the systems, distributed generators and batteries were replaced with loads with the same power levels. As a result, the test systems used here have one generator that supplies all the power demanded by the system. Said generator is located at Node 1, that is, the slack node. This section presents all the electrical characteristics and parameters of the two test systems.

4.1. 10 nodes test system

The 10 nodes test system is presented in Fig. 3. It is can be observe that this electrical system is composes for 10 buses and 9 branches [2], whit a unique generator and radial structure. The parameters of this system are show in Table 1 (see Figs. 4 and 5).

The system considers two types of loads: constant power loads (P) and resistive loads (R), which produces an initial power loss of 0.1436 p. u. for a total demand of 3.6 p.u. Finally, the voltage and power bases used in this system are 1 kV and 100 kW, respectively.

4.2. 21 nodes test system

The 21 nodes test system is presented in Ref. [24]. In Ref. [21], the authors adapted this system to conduct tests in DC. This system, composed of 21 buses and 20 lines, includes only constant power loads. Its electrical configuration is presented in Fig. 9, and its parameters are detailed in Table 2.

Table 2 shows the following data of the 21-bus test system (from left to right): transmitting bus (from), receiving bus (to), resistance (R[pu]) of the line connecting those buses, and power demand at that bus (P [pu]).

In the 21-bus test system, the slack node (Node 1) generates 5.8160 p.u. in its initial state. Besides, the voltage at the slack node is considered to be flat, that is, 1 p.u. The power losses in the system equal 0.27603 p. u. A voltage and a base power of 1 kV and 100 kW, respectively, are assumed in this system. Data about the actual power and voltage in this system are available to validate the results in case real values are required. DGs were located in the system considering a state-of-the-art review and previous studies that have produced outstanding results. Therefore, the DGs were located at nodes 9, 12, and 16, as shown in [25].

4.3. 69 nodes test system

The 69 nodes test system is an adaptation of the classical AC 69-node test system employed for power loss reduction via distributed generation integration in AC networks, presented in Refs. [4,26,27]. The base values used in this system to obtain p.u. values are 12.66 kV and 100 kVA. Additionally, modifications to the electrical configuration were made in this study, as shown in Fig. 10. The parameters of this test system are detailed in Table 3. Initially, in the 69-bus test system, the power generation of the slack node is 40.4311 p.u., and the power losses equal 1.5385 p.u. The slack node operates with a voltage of 1 p.u. In this system, the generators are located at nodes 26, 61, and 66, as reported in Ref. [13] (see Table 4).

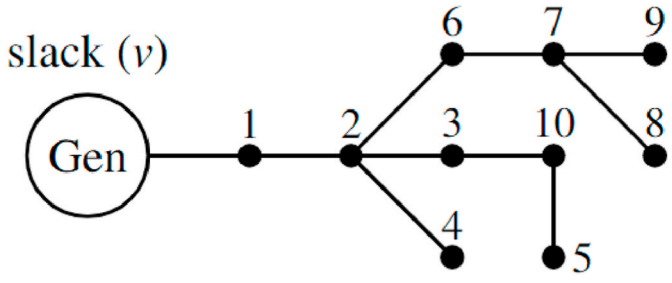

Fig. 3. Electrical configuration of the 10 nodes test system.

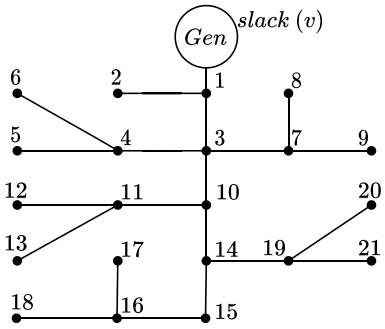

Fig. 4. Electrical configuration of the 21-bus test system.

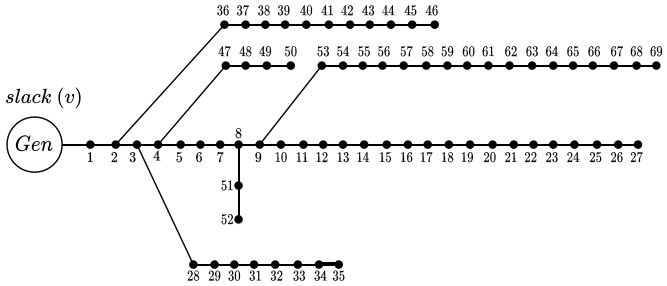

Fig. 5. Electrical configuration of the 69-bus test system.

Table 1
Electrical parameters of the 10 nodes test system.

From	To	R [pu]	P [pu]	R [pu]
1(slack)	2	0.0050	0	0
2	3	0.0015	−0.8	0
2	4	0.0020	−1.3	0
4	5	0.0018	0.5	0
2	6	0.0023	0	2.0
6	7	0.0017	0	0
7	8	0.0021	0.3	0
7	9	0.0013	−0.7	0
3	10	0.0015	0	1.25

Table 2
Electrical parameters of the 21 nodes test system.

From	To	R [pu]	P [pu]	From	To	R [pu]	P [pu]
1(slack)	2	0.0053	−0.70	11	12	0.0079	−0.68
1	3	0.0054	0.00	11	13	0.0078	0.10
3	4	0.0054	−0.36	10	14	0.0083	0.00
4	5	0.0063	−0.04	14	15	0.0065	0.22
4	6	0.0051	0.36	15	16	0.0064	−0.23
3	7	0.0037	0.00	16	17	0.0074	0.43
7	8	0.0079	−0.32	16	18	0.0081	−0.34
7	9	0.0072	0.80	14	19	0.0078	0.09
3	10	0.0053	0.00	19	20	0.0084	0.21
10	11	0.0038	−0.45	19	21	0.0082	0.21

4.4. Comparison of methods and parameters

To assess the convergence of the proposed optimization method (AOA), we compared its results to those of four other optimization methods reported in the literature, which were selected thanks to their performance in terms of quality and computation times. In sum, five methods were compared here: AOA, ALO, black hole optimization

Table 3
Electrical parameters of the 69 nodes test system.

From	To	R[pu]	P[pu]	From	To	R[pu]	P[pu]	From	To	R[pu]	P[pu]
1	2	0.0005	0	24	25	0.7488	0	47	48	0.0851	−0.79
2	3	0.0005	0	25	26	0.3089	−0.14	48	49	0.2898	−3.84
3	4	0.0015	0	26	27	0.1732	−0.14	49	50	0.0822	−3.84
4	5	0.0215	0	3	28	0.0044	−0.26	8	51	0.0928	−0.405
5	6	0.3660	−0.026	28	29	0.0640	−0.26	51	52	0.3319	−0.036
6	7	0.3810	−0.404	29	30	0.3978	0	9	53	0.1740	−0.0435
7	8	0.0922	−0.75	30	31	0.0702	0	53	54	0.2030	−0.264
8	9	0.0493	−0.3	31	32	0.3510	0	54	55	0.2842	−0.24
9	10	0.8190	−0.28	32	33	0.8390	−0.1	55	56	0.2813	0
10	11	0.1872	−1.45	33	34	1.7080	−0.14	56	57	1.5900	0
11	12	0.7114	−1.45	34	35	1.4740	−0.04	57	58	0.7837	0
12	13	1.0300	−0.08	3	36	0.0044	−0.26	58	59	0.3042	−1
13	14	1.0440	−0.08	36	37	0.0640	−0.26	59	60	0.3861	0
14	15	1.0580	0	37	38	0.1053	0	60	61	0.5075	−12.44
15	16	0.1966	−0.45	38	39	0.0304	−0.24	61	62	0.0974	−0.32
16	17	0.3744	−0.6	39	40	0.0018	−0.24	62	63	0.1450	0
17	18	0.0047	−0.6	40	41	0.7283	−1.02	63	64	0.7105	−2.27
18	19	0.3276	0	41	42	0.3100	0	64	65	1.0410	−0.59
19	20	0.2106	−0.01	42	43	0.0410	−0.06	65	66	0.2012	−0.18
20	21	0.3416	−1.14	43	44	0.0092	0	66	67	0.0047	−0.18
21	22	0.0140	−0.05	44	45	0.1089	−0.392	67	68	0.7394	−0.28
22	23	0.1591	0	45	46	0.0009	−0.392	68	69	0.0047	−0.28
23	24	0.3463	−0.28	4	47	0.0034	0				

Table 4
Parameters of the continuous methods employed in the master stage for the 10 nodes test system.

Method	AOA	ALO	BH	CGA	PSO
Number of particles	34	62	85	46	79
Maximum number of iterations	777	443	330	678	520
Maximum number of non-improvement iterations	91	89	55	72	83

(BHO), continuous genetic algorithm (CGA), and particle swarm optimization (PSO). Each of these five methods was used in the master stage of the proposed master-slave methodology to solve the OPF problem. In said methodology, the master stage uses the optimization algorithm to establish the power values to be injected by the DGs; in turn, the slave stage employs the SA numerical method to establish the power loads. To confirm the effectiveness of the five methods, this study used the 10, 21 and the 69 nodes test systems, which are frequently implemented in the literature for this purpose [2,4,18,24,28].

To make a fair comparison of the five methods employed here to solve the OPF problem, the optimization algorithms were tuned. Such tuning was performed using the PSO algorithm (presented in Ref. [4]) in the two bus test systems so that every method could obtain the best possible solution according to the objective function. The tuning parameters were population size, [1–100]; maximum number of iterations of each algorithm, [1–1000]; and non-improvement iterations, [1–1000]. The population in the PSO algorithm was 10 individuals, and the maximum number of iterations was 300. Finally, Tables 5 and 6 present the parameters of the five methods tuned for the 21- and 69-bus test systems, respectively. These parameters enable each optimization method to find the best solution to the OPF problem according to the objective function.

Table 5
Parameters of the continuous methods employed in the master stage for the 21 nodes test system.

Method	AOA	ALO	BH	CGA	PSO
Number of particles	64	79	67	52	49
Maximum number of iterations	783	769	317	592	679
Maximum number of non-improvement iterations	783	441	317	346	263

Table 6
Parameters of the continuous methods employed in the master stage for the 69 nodes test system.

Method	AOA	ALO	BH	CGA	PSO
Number of particles	73	77	35	40	58
Maximum number of iterations	378	182	566	622	723
Maximum number of non-improvement iterations	378	182	566	443	252

5. Simulations and results

This section presents the results obtained by the five optimization methods implemented here to solve the OPF problem in DC networks using the 10, 21 and 69 nodes test systems described in Section 4. The simulations were conducted in MATLAB R2018b running on a workstation with 16 GB of RAM, a 3.50-GHz Intel(R) Xeon (R) processor, a 446-GB solid state drive, and Microsoft Windows 10 Pro for Workstations. Each solution methodology was run 100 times to evaluate its repeatability, accuracy, and standard deviation. The results in each system are presented below.

5.1. Results in the 10-bus test system

Table 7 presents the results obtained by the proposed methodology and the optimization algorithms after performing 100 runs for each of the test scenarios. To carry out this work, each of the DGs is allowed to inject 20%, 40% and 60% of the power generation injected by the Slack generator for the base case (system without distributed generation). The table mentioned above represents the information of the 10-node DC system and is arranged as follows: in the first column is located the optimization algorithm used to obtain the solution to the OPF problem in DC networks, in the second column is the sum of the net power injected by the 3 DGs; in the third and fourth columns are the minimum P_{loss} and the average P_{loss} obtained by the optimization algorithms represented in kW, respectively. Similarly, the fourth and fifth columns show the percentage of loss reduction achieved (%) with respect to the P_{loss} of the base system. Column 5 shows the percentage of standard deviation obtained by each optimization algorithm. Finally, the sixth and seventh columns show the voltage farthest from 1 (worst voltage) and the highest current flowing through the conductor lines for the

Table 7
Results of the simulation in the 10 nodes test system.

10 nodes test system						
Ploss base case = 13.70859 kW						
Method	Total injected power [kW]	Power Losses Reduction			Worst V [p.u]	Imax [A]
		Minimum [kW]/Reduction [%]	Average [kW]/Reduction [%]	STD [%]		
20% power generation						
AOA	9.9417	13.3026/2.9615	13.3116/2.8959	0.3716	0.9763	310.9076
ALO	9.9389	13.3027/2.9606	13.3038/2.9527	0.0120	0.9763	310.9304
BH	9.9382	13.3367/2.7128	13.6645/0.3219	7.1627	0.9762	310.9548
CGA	9.9391	13.3120/2.8927	13.5043/1.4901	2.1499	0.9761	310.9358
PSO	9.9417	13.3026/2.9614	13.3021/2.9588	0.0023	0.9763	310.9083
40% power generation						
AOA	19.8834	13.0528/4.7839	13.0590/4.7384	0.1566	0.9824	230.4056
ALO	19.8711	13.0529/4.7833	13.0539/4.7760	0.0042	0.9823	230.4247
BH	19.8363	13.0757/4.6168	14.5807/-6.3619	17.8241	0.9822	230.7890
CGA	19.8442	13.0669/4.6808	22.1234/-61.3832	34.0867	0.9824	230.7215
PSO	19.8834	13.0528/4.7839	13.0529/4.7834	0.0004	0.9824	230.4063
60% power generation						
AOA	29.8252	12.9379/5.6218	12.9396/5.6099	0.0372	0.9887	150.9697
ALO	29.7475	12.9469/5.5566	12.9647/5.4268	0.6585	0.9883	151.6011
BH	29.7722	12.9482/5.5466	12.9881/5.2495	0.4408	0.9884	151.3946
CGA	29.8216	12.9371/5.6214	12.9391/5.6134	0.0048	0.9886	150.9980
PSO	29.8248	12.9379/5.6218	12.9381/5.6206	0.0086	0.9887	150.9724

system under analysis. For this system a 500 *kcmils* conductor is selected according to NTC2050.

Through Table 7 we obtain Figs. 6 and 7, through which the solutions reached by each optimization algorithm after the 100 runs are compared. In the first figure, the comparison in terms of minimum P_{loss} between the AOA and the other optimization algorithms employed to solve the OPF problem making use of the three penetration percentages of 20%, 40% and 60% are presented. For the scenario that is allowed a penetration percentage of 20%, the AOA achieves a minimum P_{loss} reduction of 2.9615%, outperforming the CGA, BH, ALO and PSO by 0.0687%, 0.2487%, and 0.0008% and 0.0001% respectively. For the case considering 40% distributed generation again the AOA is the optimization algorithm that achieves the best minimum P_{loss} reduction, achieving a reduction of 4.7839% and outperforming the other algorithms by an average percentage of 0.0677%. For the case considering the 60% power injection by the GDs, again the AOA achieves the best minimum P_{loss} reduction, achieving a reduction of 5.6218%, outperforming the PSO by 0.00004%, the CGA by 0.0005%, the ALO by 0.0653% and the BH by 0.0752%. The above analyzed results show that the AOA is the algorithm that allows obtaining the best results in terms of minimum P_{loss} reduction for the 10-node system.

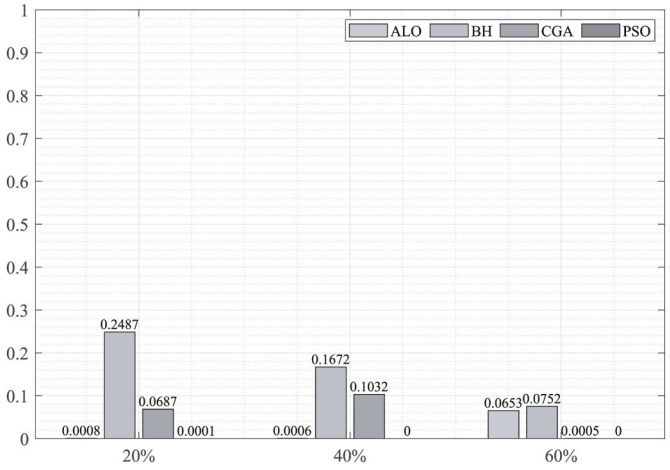

Fig. 6. Average reductions in power loss compared to AOA in the 10 nodes test system.

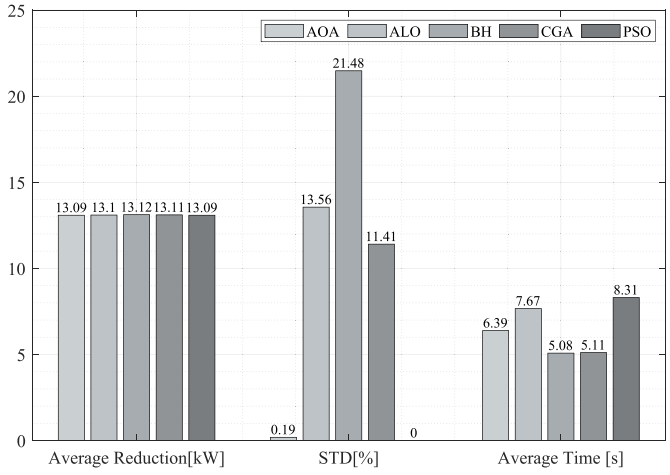

Fig. 7. Average results in the 10 nodes test system.

In Fig. 7 it is possible to appreciate the average P_{loss} reduction percentage obtained by each algorithm for the three allowed penetration percentages, as well as the standard deviation and the average time taken by each algorithm to obtain the best solution for the problem addressed. For the case considering the average P_{loss}, the AOA achieves an average reduction of 13.09 kW, tying with the PSO and being outperformed by the ALO by only 0.01 kW, by the CGA by only 0.02 kW and the BH by only 0.03 kW. For the scenario that evaluates the standard deviation, the AOA achieves an average percentage of 0.19%, being surpassed only by the PSO by 0.1899%, but in turn surpasses the CGA by 11.41%, ALO by 13.56% and the BH by 21.48%. For the case where processing times are considered, the AOA manages to solve the OPF problem for the 10-node system in an average time of 6.39*s*, being outperformed only by the BH and CGA by only 1.31*s* and 1.28*s*, respectively; but outperforming the ALO by 1.28*s* and the PSO by 1.92*s*. The results discussed above show that the AOA can obtain good solutions in terms of average P_{loss}, obtaining an excellent standard deviation for each penetration percentage, and managing to reach the solution of this system in a short average time.

5.2. Results in the 21 nodes test system

Table 8 shows the results of the five methods in the 21-bus test system with 20%, 40%, and 60% of the power injected by DGs with respect to the maximum power level injected by the slack node. This table contains seven columns (from left to right): optimization method; total power injected by the 3 DGs; minimum power losses (P_{loss}) obtained by each method [kW] and reduction in percentage compared with the base case; average P_{loss} of each method [kW] and reduction in percentage compared with the base case; standard deviation STD of each method [%]; worst voltage of the system in $p.u.$; and maximum voltage flowing through the distribution lines [A]. In the 21-bus test system, the maximum allowable voltage was 520A.

Table 8 presents the results obtained by the optimization methods in the 21 nodes test system. Figs. 8 and 9, which were obtained from said table, compare the minimum and average Ploss obtained by the five optimization algorithms. Fig. 8 compares the average minimum error in P_{loss} in the 3 DG scenarios: 20%, 40%, and 60% of the power supplied by the slack node compared to AOA. The AOA and PSO present the best responses in terms of P_{loss} reduction with 20% penetration, both achieving a 52.2382% reduction compared with the base case, thus outperforming ALO, the CGA, and BHO by 0.0039%, 0.0485%, and 0.4256%, respectively. With 40% penetration, the AOA and PSO achieved the best reductions in P_{loss}, followed by ALO, which ranks in third place with a reduction of 77.8220%, the CGA in fourth place with 77.8175%, and BHO in the fifth place with 77.6280%. With a penetration of 60%, the AOA achieved a reduction percentage of 89.9061%, which was outperformed by PSO and ALO by 0.0022% and 0.0010%, respectively. However, the AOA outperformed the CGA and BHO by 0.0153% and 0.1069%, respectively.

Fig. 9 shows the differences in average P_{loss} between the proposed optimization algorithm and the other four methods after running them 100 times. With 20% penetration, the AOA presented the best reduction in average P_{loss} with 52.2338%, thus outperforming (in this order) PSO, ALO, the CGA, and BHO by 0.1143%, 0.2983%, 0.3610%, and 3.2130%, respectively. With 40% penetration, the AOA produced the best reduction in P_{loss} with 77.7971%, thus outperforming ALO, PSO, the CGA, and BHO by 0.0014%, 0.692%, 0.0700%, and 1.4755%, respectively. With a penetration of 60%, the AOA achieved a reduction percentage of 89.8930%, which was outperformed by ALO by 0.0069%. Nevertheless, the AOA still outperformed PSO, the CGA, and BHO by 0.0439%, 0.0804% and 0.9134%, respectively.

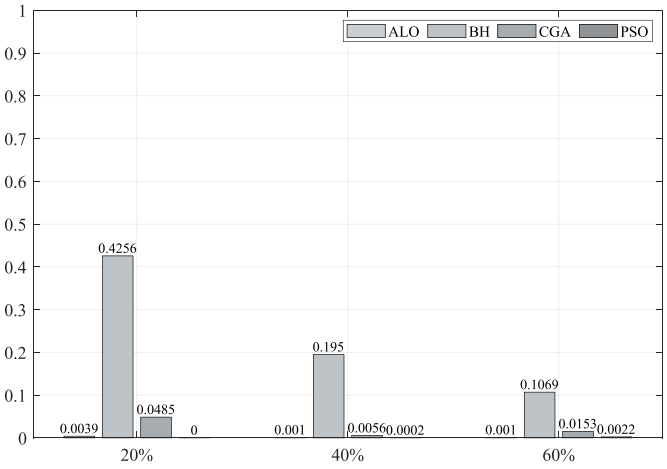

Fig. 8. Average reductions in power loss compared to AOA in the 21 nodes test system.

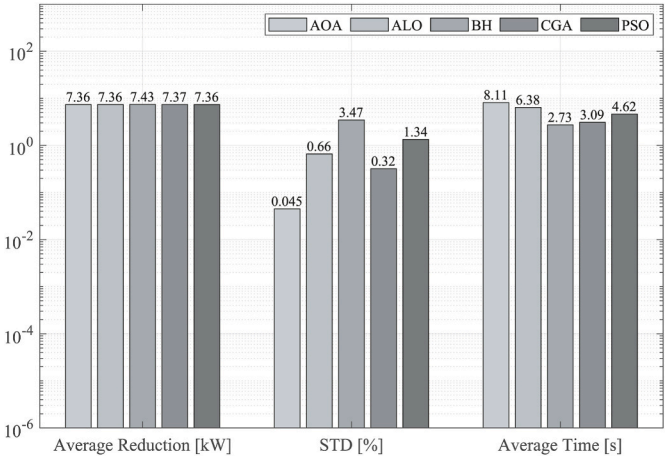

Fig. 9. Average results in the 21 nodes test system.

Table 8
Results of the simulation in the 21 nodes test system.

21 nodes test system						
Ploss base case = 27.603 kW						
Method	Total injected power [kW]	Power Losses Reduction			Worst V [p.u]	Imax [A]
		Minimum [kW]/Reduction [%]	Average [kW]/Reduction [%]	STD [%]		
20% power generation						
AOA	116.3207	13.1823/52.2382	13.1835/52.2338	0.0058	0.9570	380.6000
ALO	116.3176	13.1833/52.2343	13.2658/52.9356	1.1400	0.9571	380.6041
BH	116.3182	13.2997/51.8126	14.0703/49.0208	2.4181	0.9543	380.7199
CGA	116.1763	13.1957/52.1896	13.2831/51.8728	0.2787	0.9570	380.7577
PSO	116.3207	13.1823/52.2382	13.2150/52.1195	0.7833	0.9571	380.5999
40% power generation						
AOA	232.6400	6.1208/77.8230	6.1280/77.7971	0.0554	0.9713	257.21920
ALO	232.6348	6.1211/77.8220	6.1284/77.7957	0.8002	0.9713	257.22470
BH	232.1035	6.1747/77.6280	6.5352/76.3216	3.2377	0.9702	257.80950
CGA	232.6327	6.1224/77.8175	6.1473/77.7271	0.2356	0.9711	257.22800
PSO	232.6414	6.1208/77.8232	6.1471/77.7279	1.2434	0.9713	257.21780
60% power generation						
AOA	348.9243	2.7859/89.9061	2.7895/89.8930	0.0744	0.9823	137.6000
ALO	348.9581	2.7856/89.9071	2.7876/89.8999	0.0436	0.9823	137.5959
BH	347.1716	2.8154/89.7992	3.0416/88.9795	4.7602	0.9820	139.3822
CGA	348.8699	2.7902/89.8907	2.8117/89.8126	0.4493	0.9827	137.6587
PSO	348.9620	2.7853/89.9083	2.8017/89.8491	2.0068	0.9824	137.5616

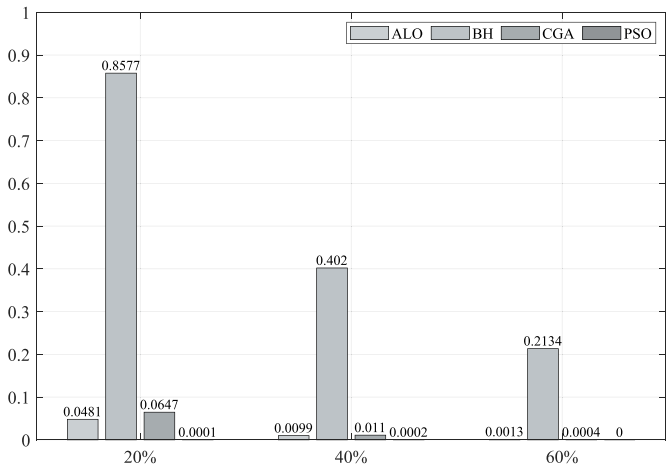

Fig. 10. Average reductions in power loss compared to AOA in the 69 nodes test system.

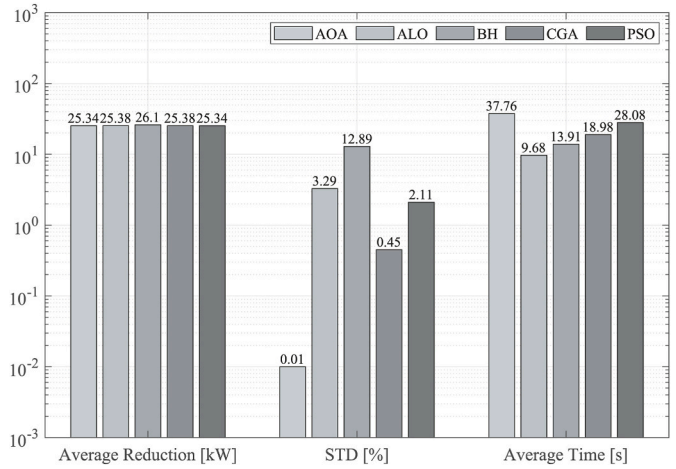

Fig. 11. Average results in the 69 nodes test system.

To assess the repeatability and precision of the optimization algorithms in solving the OPF problem in the 21 nodes test system, Fig. 9 compares the standard deviation of the proposed optimization method with those of the other four optimization algorithms. With 20% power injection, the AOA presents the best standard deviation, i.e., 0.0058%, outperforming the CGA by 0.2729%, PSO by 0.7775%, ALO by 1.1341%, and BHO by 2.4123%. With 40%, the AOA achieved the best standard deviation again with 0.055%, thus outperforming the CGA, ALO, PSO, and BHO by 0.1802%, 0.7448%, 1.1880%, and 3.1824%, respectively. With 60%, the AOA obtained a standard deviation of 0.074%, outperformed only by ALO by 0.030%. In this scenario, the AOA outperformed the CGA by 0.375%, PSO by 1.932%, and BHO by 4.686%.

5.3. 69 nodes test system

Table 9 presents the results obtained by each optimization algorithm analyzed in the 69 nodes test system, where the DGs were enabled to inject 20%, 40%, and 60% of the power supplied by the slack node. It is organized as Table 8, but the maximum allowable current was 335A in this case. The results presented in Table 9 are illustrated in Figs. 10 and 11, which compare the minimum and average P_{loss} of the AOA with those of the other four optimization algorithms.

Fig. 10 shows the difference in average minimum error in P_{loss} with 20%, 40%, and 60% of DG injection compared to AOA. In this figure, with 20% injection, the AOA presented the best solution to the OPF problem with a reduction of 63.2854%, outperforming PSO by 0.0001%, ALO by 0.0481%, the CGA by 0.647%, and BHO by 0.8577%. With 40% injection, PSO showed a reduction of 90.9048%, outperforming the AOA by 0.0001%, followed by ALO, the CGA, and BHO with 90.8948%, 90.8936%, and 90.5027%, respectively. With 60%, the AOA and PSO obtained the best value in P_{loss} reduction, i.e., 96.3888% each, followed by the CGA with 96.3884%, ALO with 96.3876%, and BHO with 96.1755%.

Fig. 11 shows the differences in average P_{loss} between the AOA and the other four optimization algorithms. In the 20% scenario, the AOA exhibited the best average power loss reduction, i.e., 63.2840%, outperforming PSO, the CGA, ALO, and BHO by 0.1392%, 0.3867%, 0.5924%, and 3.7985%, respectively. With 40% power injection, the AOA presented the best P_{loss} average reduction with 90.9021%, followed by the CGA with 90.8006%, PSO with 90.6968%, ALO with 90.8948%, and BHO with 87.8768%. With 60% power injection, the AOA and PSO showed a reduction of 96.3888%, outperforming the CGA by 0.0156%,

Table 9
Results of the simulation in the 69 nodes test system.

69 nodes test system						
Ploss base case = 115.855 kW						
Method	Total injected power [kW]	Power losses Reduction			Worst V [p.u]	Imax [A]
		Minimum [kW]/Reduction [%]	Average [kW]/Reduction [%]	STD [%]		
20% power generation						
AOA	808.6190	56.4854/63.2854	54.4876/63.2740	0.0015	0.9610	247.7975
ALO	808.2789	56.5594/63.2373	57.3990/62.6916	1.1593	0.9607	247.8302
BH	802.5487	57.805/62.4277	62.3316/59.4855	4.4940	0.9616	248.3812
CGA	807.9075	56.5850/63.2207	57.0826/62.8972	0.4181	0.9606	247.8616
PSO	808.6195	56.4856/63.2853	56.7017/63.4848	0.4072	0.9610	247.7975
40% power generation						
AOA	1617.0000	13.9931/90.9047	13.9971/90.9021	0.0164	0.9847	180.57120
ALO	1616.8836	14.0084/90.8948	14.4271/90.6226	2.3783	0.9846	180.59830
BH	1604.0404	14.6116/90.5027	18.6515/87.8768	12.6229	0.9840	181.66040
CGA	1616.9396	14.0101/90.8936	14.1533/90.8006	0.6437	0.9847	180.59400
PSO	1617.2390	13.9929/90.9048	14.3129/90.6968	5.9359	0.9847	180.56900
60% power generation						
AOA	2209.3127	5.5558/96.3888	5.5558/96.3888	0.0000	0.9949	133.1353
ALO	2215.5314	5.7315/96.3876	5.7315/96.2746	6.3320	0.9950	132.6443
BH	2162.1432	5.8840/96.1755	8.3247/94.5891	21.5430	0.9950	136.8871
CGA	2204.7900	5.5565/96.3884	5.5797/96.3733	0.2977	0.9949	133.4926
PSO	2209.3229	5.5558/96.3888	5.5558/96.3888	0.0000	0.9949	133.1345

ALO by 0.1142%, and BHO by 1.7997%.

As with the 21 nodes test system, Fig. 11 shows the differences in standard deviation between the AOA and the other four optimization methods in the 69-bus system. This figure can be used to evaluate the accuracy and repeatability of each method in finding a good quality solution. As shown in Fig. 11, the AOA presented the best standard deviation with 20% penetration, i.e., 0.0015%, thus outperforming PSO by 0.4057%, the CGA by 0.4166%, ALO by 1.1578%, and BHO by 4.4925%. With 40% DG, the AOA exhibited a standard deviation of 0.0164%, outperforming the other optimization algorithms by an average of 5.3788%. With 60% penetration, the AOA obtained a standard deviation of 3.94×10^{-6}, which was outperformed by PSO by only 3.35×10^{-6}. However, the AOA outperformed the CGA by 0.2977%, ALO by 6.3320%, and BHO by 21.5430%. This analysis proves that the AOA method is the best option for obtaining a high quality solution every time the algorithm is run.

6. Conclusions

This article presented a new optimization method for the Optimal Power Flow (OPF) problem in Direct Current (DC) networks using a master-slave methodology. In the latter, the master stage is performed by the Arithmetic Optimization Algorithm (AOA), which evaluates possible solutions to the OPF problem considering its constraints. Subsequently, the slave stage evaluates the fitness of the solutions to the problem (proposed by its master counterpart) and uses Successive Approximations (SA) to solve the OPF problem. Three scenarios, two systems, and four other methods were implemented to validate the proposed methodology. The three scenarios were defined to evaluate the performance of the algorithms when the power injected by DGs was limited to 20%, 40%, and 60% with respect to the power injected by the slack node. The 21- and 69-bus test systems, frequently reported in the literature, were also employed for this validation.

The results allow us to conclude that the AOA-SA method proposed in this article is the best option to solve the OPF problem because it achieves the best standard deviation (as shown in the figures and tables above) in the solution to the OPF problem. Thus, this method is the most likely to produce an optimal solution in terms of power supplied by each generator and significant reductions in power losses.

The figures also show that the reductions in power losses obtained by the methods do not present significant differences. However, if we analyze them in terms of kilowatts or megawatts, it is evident that the most efficient method, that is, the proposed method, can reduce power losses, thus generating significant savings. The tables indicate that this method (i.e., AOA-SA) also kept the voltage and current within their limits, which is a good indicator of its performance and also proves that the constraints of the OPF problem were respected.

Credit author statement

conceptualization, methodology, formal analysis, investigation, and writing-original draft preparation, Jhon Montano, Oscar Daniel Garzon, and Luis Fernando Grisales-Noreña. Writing-original draft preparation Jhon Montano, Oscar Daniel Garzón, Andres Alfonso Rosales Muñoz, Luis Fernando Grisales-Noreña, and Oscar Danilo Montoya.

Declaration of competing interest

The authors declare that they have no known competing financial interests or personal relationships that could have appeared to influence the work reported in this paper.

Acknowledgments

This research and the APC were funded by Minciencias through the \textit{Fondo Nacional de Financiamiento para la Ciencia, la Tecnología y la Innovación, Fondo Francisco José de Caldas}; Instituto Tecnológico Metropolitano; Universidad Nacional de Colombia; and Universidad del Valle under the Project entitled “Estrategias de dimensionamiento, planeación y gestión inteligente de energía a partir de la integración y la optimización de las fuentes no convencionales, los sistemas de almacenamiento y cargas eléctricas, que permitan la generación de soluciones energéticas confiables para los territorios urbanos y rurales de Colombia”, which is part of the research program entitled “Estrategias para el desarrollo de sistemas energéticos sostenibles, confiables, eficientes y accesibles para el futuro de Colombia”.

References

[1] O. Garzon-Rivera, J. Ocampo, L. Grisales-Noreña, O. Montoya, J. Rojas-Montano, Optimal power flow in direct current networks using the antlion optimizer, Statist. Optimizat. Informat. Comput. 8 (4) (2020) 846–857.
[2] A. Garces, Uniqueness of the power flow solutions in low voltage direct current grids, Elec. Power Syst. Res. 151 (2017) 149–153.
[3] O.D. Montoya, W. Gil-González, V.M. Garrido, Voltage stability margin in dc grids with cpls: a recursive Newton–raphson approximation, IEEE Transact. Circuits Syst. II: Express Briefs 67 (2) (2019) 300–304.
[4] L.F. Grisales-Noreña, D. Gonzalez Montoya, C.A. Ramos-Paja, Optimal sizing and location of distributed generators based on pbil and pso techniques, Energies 11 (4) (2018) 1018.
[5] O.D. Montoya, D.A. Giral-Ramírez, L.F. Grisales-Noreña, Optimal economic-environmental dispatch in mt-hvdc systems via sine-cosine algorithm, Results Eng. 13 (2022), 100348.
[6] L.F. Grisales-Noreña, O.D. Montoya, W.J. Gil-González, A.-J. Perea-Moreno, M.-A. Perea-Moreno, A comparative study on power flow methods for direct-current networks considering processing time and numerical convergence errors, Electronics 9 (12) (2020) 2062.
[7] L.F. Grisales-Noreña, O.D. Montoya, C.A. Ramos-Paja, An energy management system for optimal operation of bss in dc distributed generation environments based on a parallel pso algorithm, J. Energy Storage 29 (2020), 101488.
[8] P. Rault, X. Guillaud, F. Colas, S. Nguefeu, Investigation on Interactions between Ac and Dc Grids, in: 2013 IEEE Grenoble Conference, IEEE, 2013, pp. 1–6.
[9] O.D. Montoya, W. Gil-González, L. Grisales-Noreña, An exact minlp model for optimal location and sizing of dgs in distribution networks: a general algebraic modeling system approach, Ain Shams Eng. J. 11 (2) (2020) 409–418.
[10] O.D. Montoya, A convex opf approximation for selecting the best candidate nodes for optimal location of power sources on dc resistive networks, Engineering Science and Technology, Int. J. 23 (3) (2020) 527–533.
[11] N. Chaudhuri, B. Chaudhuri, R. Majumder, A. Yazdani, Multi-terminal Direct-Current Grids: Modeling, Analysis, and Control, John Wiley & Sons, 2014.
[12] E. Prieto-Araujo, A. Egea-Alvarez, S. Fekriasl, O. Gomis-Bellmunt, Dc voltage droop control design for multiterminal hvdc systems considering ac and dc grid dynamics, IEEE Trans. Power Deliv. 31 (2) (2015) 575–585.
[13] L.F. Grisales-Noreña, D. Gonzalez Montoya, C.A. Ramos-Paja, Optimal sizing and location of distributed generators based on pbil and pso techniques, Energies 11 (4) (2018) 1018.
[14] L. F. Grisales-Noreña, O. D. Garzón Rivera, J. A. Ocampo Toro, C. A. Ramos-Paja, M. A. Rodriguez Cabal, Metaheuristic Optimization Methods for Optimal Power Flow Analysis in Dc Distribution Networks.
[15] J. Li, F. Liu, Z. Wang, S.H. Low, S. Mei, Optimal power flow in stand-alone dc microgrids, IEEE Trans. Power Syst. 33 (5) (2018) 5496–5506.
[16] O.D. Montoya, W. Gil-González, A. Garces, Sequential quadratic programming models for solving the opf problem in dc grids, Elec. Power Syst. Res. 169 (2019) 18–23.
[17] O. Montoya, W. Gil-González, L. Grisales-Noreña, Optimal Power Dispatch of Dgs in Dc Power Grids: A Hybrid Gauss-Seidel-Genetic-Algorithm Methodology for Solving the Opf Problem.
[18] A.A. Rosales-Muñoz, L.F. Grisales-Noreña, J. Montano, O.D. Montoya, A.-J. Perea-Moreno, Application of the multiverse optimization method to solve the optimal power flow problem in direct current electrical networks, Sustainability 13 (16) (2021) 8703.
[19] J. Giraldo, O. Montoya, L. Grisales-Noreña, W. Gil-González, M. Holguín, Optimal power flow solution in direct current grids using sine-cosine algorithm, in: Journal of Physics: Conference Series vol. 1403, IOP Publishing, 2019, 012009.
[20] O.S. Velasquez, O.D. Montoya Giraldo, V.M. Garrido Arevalo, L.F. Grisales Norena, Optimal power flow in direct-current power grids via black hole optimization, Adv. Electric. Electron. Eng. 17 (1) (2019) 24–32.
[21] O.D. Montoya, L.F. Grisales-Noreña, D. González-Montoya, C. Ramos-Paja, A. Garces, Linear power flow formulation for low-voltage dc power grids, Elec. Power Syst. Res. 163 (2018) 375–381.
[22] L. Abualigah, A. Diabat, S. Mirjalili, M. Abd Elaziz, A.H. Gandomi, The arithmetic optimization algorithm, Comput. Methods Appl. Mech. Eng. 376 (2021), 113609.
[23] O.D. Montoya, V.M. Garrido, W. Gil-González, L.F. Grisales-Noreña, Power flow analysis in dc grids: two alternative numerical methods, IEEE Transact. Circuits Syst. II: Express Briefs 66 (11) (2019) 1865–1869.
[24] A. Garcés, On the convergence of Newton’s method in power flow studies for dc microgrids, IEEE Trans. Power Syst. 33 (5) (2018) 5770–5777.

[25] O.S. Velasquez, O.D. Montoya Giraldo, V.M. Garrido Arevalo, L.F. Grisales Norena, Optimal power flow in direct-current power grids via black hole optimization, Adv. Electric. Electron. Eng. 17 (1) (2019) 24–32.
[26] S. Kaur, G. Kumbhar, J. Sharma, A minlp technique for optimal placement of multiple dg units in distribution systems, Int. J. Electr. Power Energy Syst. 63 (2014) 609–617.
[27] S. Sultana, P.K. Roy, Krill herd algorithm for optimal location of distributed generator in radial distribution system, Appl. Soft Comput. 40 (2016) 391–404.
[28] W. Gil-González, O.D. Montoya, E. Holguín, A. Garces, L.F. Grisales-Noreña, Economic dispatch of energy storage systems in dc microgrids employing a semidefinite programming model, J. Energy Storage 21 (2019) 1–8.